Local triplet superconductivity of $La_{0.65}Ca_{0.35}MnO_3$-X point contacts (X=Pb,MgB_2)

V. N. Krivoruchko and V. Yu. Tarenkov

Donetsk Physics and Technology Institute, NAS of Ukraine, 72 R. Luxemburg Street, 83114 Donetsk, Ukraine
(Received 26 July 2006; revised manuscript received 23 March 2007; published 14 June 2007)

Microconstrictions between spin-singlet superconductor, Pb or MgB_2, tip and half-metallic ferromagnet, $La_{0.65}Ca_{0.35}MnO_3$ (LCMO), plate have been realized by means of a point-contact inset. Measurements of the current-voltage characteristics and of the dynamic conductance $G(V)$ versus bias have been performed to probe mutual influence of superconductivity and half-metallic ferromagnetism. In the contacts, which we distinguish as proximity affected ones, a few principal effects have been observed. Namely, with decreasing temperature, a spectacular drop of the contact's resistance has been detected with an onset of the Pb or MgB_2 superconductivity; for small voltages, an excess current and doubling of the normal-state conductance have also been found. We conclude that the underlying physical explanations for these results are the conversion from spin-singlet pairs to spin-triplet ones at the Pb (MgB_2)/LCMO interface and a long-range proximity induced superconductivity of LCMO. Superconducting state of LCMO is also supported by the observation of the coherent multiple Andreev reflections (subharmonic gap resonances). We also found that the character of $G(V)$ vs voltage dependence corresponds to that for the induced superconducting energy gap of LCMO much larger than that of Pb or MgB_2. All specific characteristics of proximity affected contacts suggest that the local triplet superconducting fluctuations are essentially sustained in LCMO and the singlet superconductors only fix the phase coherency of a superconducting state.

I. INTRODUCTION

At energies below the superconducting gap, a charge transport through a normal metal/superconductor (N/S) contact is possible only by Andreev reflection (AR) process.[1] That is, when an electron reaches an S/N interface, it cannot enter into the superconducting region if its energy E is smaller than the superconducting energy gap. It is then backscattered as a hole with energy $-E$. These electron and the hole are coherently coupled, i.e., the phase-coherent electron-hole conversion results in a nonzero pair amplitude in the normal metal, creating a weakly superconducting region at the metal/superconductor interface. An alternative but equivalent way of thinking about AR processes is through a proximity effect (PE). The superconducting proximity region has a lower transition temperature and a lower superconducting energy gap Δ than the bulk. It is important to emphasize that the superconducting PE is characteristic not only for S/N layered structures but for *most S/N point contacts* as well (see, for example, Ref. 2 and references therein). Blonder *et al.*[3] showed that the charge doubling at the interface enhances the subgap conductance and this phenomenon has indeed been observed in the case of a perfectly transparent interface. For our further discussion, it is also significant that an important advantage of point-contact (PC) method is that the order parameter varies on the scale of the PC diameter, which typically is much smaller than the superconducting coherence length. Therefore, the excess current of a PC contains information about the position dependence of the superconducting order parameter near the interface.

The picture of proximity effect is significantly modified when spin comes into play. If the N is a ferromagnet, there is an imbalance between spin-up and spin-down populations, which suppresses the AR and reduces the subgap conductance below the normal-state value. Theory predicts that in the extreme case of a completely spin-polarized material being in contact with a conventional (singlet s-wave pairing) S, the PE is absent.[4] Therefore, one might expect that the influence of the superconducting PE on the transport properties of a S/half-metallic ferromagnet (HMF) heterostructure should be negligibly small.

However, researches of the last decade suggested that a superconducting proximity effect may be a characteristic feature for superconductor/ferromagnet (S/F) structures as well. Namely, a growing number of experimental evidences promote conclusion that an unconventional long-distance PE may be realized in S/F point contacts, nanowires, etc. Kasai *et al.*[5] were the first, to our best knowledge, who asserted this hypothesis based on the results of the investigation of current-voltage characteristics for $YBa_2Cu_3O_y$/magnetic manganese oxide/$YBa_2Cu_3O_y$ trilayers. For certain cases, the authors observed that supercurrent passes through manganese oxide layers ($La_{1-x}Ca_xMnO_z$ or $La_{1-x}Sr_xMnO_z$) up to 200 nm thickness. These results cannot be explained within the framework of the conventional PE and a novel type of the PE related with magnetism of the barrier has been suggested. Recently, there have been speculations of a few groups[6–8] concerning unconventional mutual influence of superconducting and ferromagnetic orders in hybrid S/F metallic nanostructures (see also review[9]). Most recently, Keizer *et al.*[10] detected a Josephson supercurrent between two S electrodes through the HMF CrO_2 layers up to 310 nm thickness. The results were explained assuming a conversion from spin-singlet pairs to spin-triplet ones at S/HMF interface and long-range PE.

However, the existing experimental evidences supporting unconventional PE in S/F structures are scarce and controversial. The phenomenon still remains unclear and requires clear-cut experimental evidences.

Recently, we addressed the problem of interplay between a singlet superconductivity and subgap spin-polarized cur-

rent in singlet superconductor (sS)/HMF microstrictions. Measurements of the current-voltage characteristics (*I-V*) and of the dynamic conductance $dI/dV=G(V)$ versus bias voltage have been performed for Pb/La$_{0.65}$Ca$_{0.35}$MnO$_3$ (LCMO) point contacts.[11] Our motivation was that if the conversion from singlet to triplet pairing exists in sS/HMF heterostructures, the sS/HMF PCs have to reveal distinct features typical for sS/N contacts such as excess current and doubling of the normal-state conductance, which have not yet been demonstrated in experiment until now. Indeed, for some of the contacts the measured AR spectrum displays very distinct characteristics which we interpret as the manifestation of an unconventional PE.

This paper is a follow up paper and focuses on three objects. Firstly, we will present the experimental results that have been obtained on PCs with qualitatively another superconducting material, MgB$_2$, used as the sS electrode (MgB$_2$/LCMO PCs). A comparison of the data obtained on PCs with different sS electrodes (Pb and MgB$_2$) will be made and some details that were forcedly omitted by a Letter format will be discussed. In particular, we will point out a (robust) feature that tells the difference between the proximity affected contacts and the contacts "without proximity effect." Secondly, we will focus on a subharmonic gap structure (SGS) that has been observed in the AR spectra. According to modern models, the origin of the SGS is due to coherent multiple Andreev reflections and it can only occur in metallic constrictions where both electrodes are in a superconducting state.[12] Thirdly, possible physical mechanisms behind the PE and spin-polarized Andreev current in LCMO/(Pb,MgB$_2$) PCs will be discussed. We argue in favor of the supposition that (at low temperature) the LCMO is thermodynamically very close to a *p*-wave triplet superconducting state, whereas the proximity induced correlations only quench the superconducting phase fluctuations.

The structure of the paper is as follows. Section II is devoted to the experimental details. In Sec. III, the data obtained on MgB$_2$/LCMO proximity affected contacts are expounded. We also make a comparison with the results on proximity Pb/LCMO junctions partially published in Ref. 11. Discussion of the experimental results and comparison to models of a subgap transport in sS/HMF structures are presented in Sec. IV. We end with the summary in Sec. V.

II. EXPERIMENTAL DETAILS

Current-voltage characteristic (*I-V*) and conductance spectra (dI/dV vs V) were measured by using a homebuilt point-contact setup operating from liquid-helium temperature to room temperature. The samples were prepared as follows. High quality textured LCMO plates were grown using standard ceramic technique. The ceramic powder plates sized $0.1 \times 1 \times 10$ mm^3 were pressed (20 kbar) and then subjected to an annealing for 8 h at 1200–1250 °C. This leads to an increase of the average size values of crystallites up to values about 5–10 μm. Temperature dependence of the plate's resistance has a sharp maximum near $T_{Curie} \approx 270$ K associated with the well known metal-dielectric transition.[13,14] Below room temperature, the resistance of the plates was ~ 1 Ω.

The low-field ($H \approx 100$ Oe) magnetoresistive effect $[\rho(T,0) - \rho(T,H)]/\rho(T,0)$ at $T=77$ K was only 0.3%. This aspect suggests that the contribution of intergranular junctions to the total sample resistance is negligibly small and confirms high quality of the ceramic plates.

Metallic contacts between LCMO plate and superconducting tip were formed by pressing slide-squash up a tip-shaped superconductor against the LCMO surface. As a superconducting electrode, we used two low-temperature superconductors with different superconducting parameters: Pb and MgB$_2$. For further references, let us note here that for Pb we have the critical temperature $T_C=7.2$ K, the energy gap $\Delta_{Pb}=1.41$ mV, the superconducting correlation length $\xi_S=830$ Å, while for two-gap MgB$_2$ these parameters are $T_C=37$ K, $\Delta_p=2.0$–2.8 mV, $\Delta_\sigma=7.0$–7.5 mV and $\xi_S=25$, and 65 Å (see, e.g., Ref. 15). The contacts were made at room temperature and at liquid nitrogen, as well, but the results did not depend upon the way of preparation. The contacts' parameters were stable, offering a possibility to perform measurements in a wide temperature range. Note that in comparison to manganites/high-T_C S structures in our contacts, the so-called hole-charge transfer effect[16] is absent.

The current-voltage (*I* vs *V*) characteristics were measured by using a conventional four-probe method. Resistivity as a function of temperature was measured directly by using an ac voltage bias source with a small output resistance and ~ 400 μV amplitude of the signal on the sample. To record the AR spectra (dI/dV vs V) of the point contacts, we used 150–200 μV modulating ac voltage. The resistance of the current and potential contacts was $R \sim 10^{-4}$ Ω cm^2. The junction resistance was much larger (~ 100 Ω), so that the rescaling effects can be neglected. The distance between the outer contacts (at LCMO surface) and superconducting terminal was not less than 2–3 mm.

We estimated the effective value of the contact diameter d by employing the Wexler formula:[17]

$$R_N \approx \frac{4}{3\pi} \frac{\rho l}{d^2} + \frac{\rho}{2d}, \tag{1}$$

where ρ is the specific resistance and l is a mean free path. We restored the charge-carrier mean free path l in LCMO by employing the known relation for conductivity σ:

$$\sigma = e^2 N(E_F)D, \quad D = l v_F/3. \tag{2}$$

Here, D is the diffusion coefficient, $N(E_F)$ stands for the charge-carrier density of states at the Fermi surface, and v_F is the Fermi velocity. For high quality films of La$_{1-x}$Ca$_x$MnO$_3$ (with $x=0.3$–0.5), a typical value of $\rho(T=4.2$ K) is $\sim(100$–$150)\times10^{-6}$ Ω cm.[18] For the estimations we took $\rho \sim 10^{-4}$ Ω cm. Using also the results obtained in Ref. 19, we choose $v_F^\uparrow=7.4\times10^7$ cm/s and $N_\uparrow(E_F)=0.58$ eV^{-1} (per Mn ion) for spin-up itinerant electrons. By employing these data, from Eq. (2) we obtain $l \sim 100$ Å. For the contacts with $R_N \sim 100$ Ω and $l \sim 100$ Å, Eq. (1) gives for the effective contact's diameter $d \sim 100$ Å. (Of course, the mechanical constriction area is much larger than the region with metallic conductivity.) Thus, we deal with the so-called Sharvin contacts.[20] The relation $d \sim l$ also means that charge transport
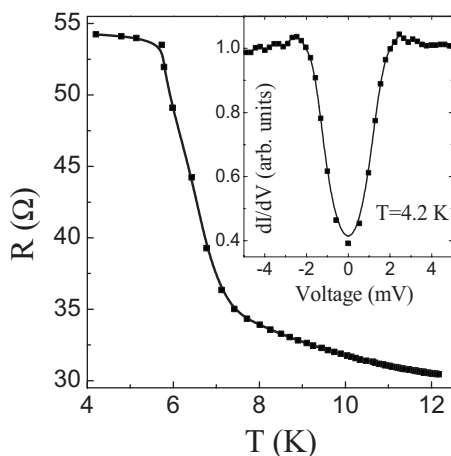
FIG. 1. Typical temperature dependence of a resistance of Pb/LCMO contact "without proximity effect." Inset: Typical Andreev reflection spectra for Pb/LCMO point contact without proximity effect.

regime in the contacts is intermediate, i. e., neither a diffusive ($d \gg l$) nor a ballistic ($d \ll l$) one.

III. RESULTS

In total, we prepared about 200 samples and recorded their AR spectra. In most cases (about 80% of samples), the contacts reveal properties that reflect the half-metallic nature of LCMO (see, for example discussion, in Ref. 21). Typically, the resistivity of these PCs was three to five times lower than those of the proximity affected contacts. A fingerprint of the contacts without proximity effect is a quite visible *increase* of the contact's resistivity just after superconducting transition temperature of the electrode (Pb or MgB$_2$). In Fig. 1 (main panel), a representative low-temperature-region behavior of the resistivity of Pb/LCMO PC without proximity effect is shown. Below T_C(Pb)=7.2 K, we observe almost doubling of the contact's resistivity. The inset in Fig. 1 demonstrates the typical spectroscopic characteristics of Pb/LCMO contact without proximity effect. Any visible features of a superconducting PE have not been detected here. For singlet pairing in the dirty limit, superconducting coherence length is $\xi_F = (\hbar D / k_B \pi T_{Curie})^{1/2}$ (see, for example, Ref. 9) and for LCMO one can obtain an extremely short distance ~ 5–7 Å. Contribution of such a small region to the contact's resistance is less than 1%. The results we have obtained on the contacts without PE can be found in Ref. 22.

For some of the cases, the measured contact's spectra reveal very distinct features which we interpret as the manifestation of an unconventional PE. The resistivity of proximity affected contacts was typically larger than that for the contacts without proximity effect. We connect this with some specific conditions that have to be fulfilled in order to transform a zero-spin Cooper pair into a triplet equal-spin pair. As will be discussed below (see Sec. IV), for this transformation the S/F interface should be "spin active," i.e., in the ferromagnet there must be an additional scattering processes to transform spin-singlet pairs into triplet ones. It might be
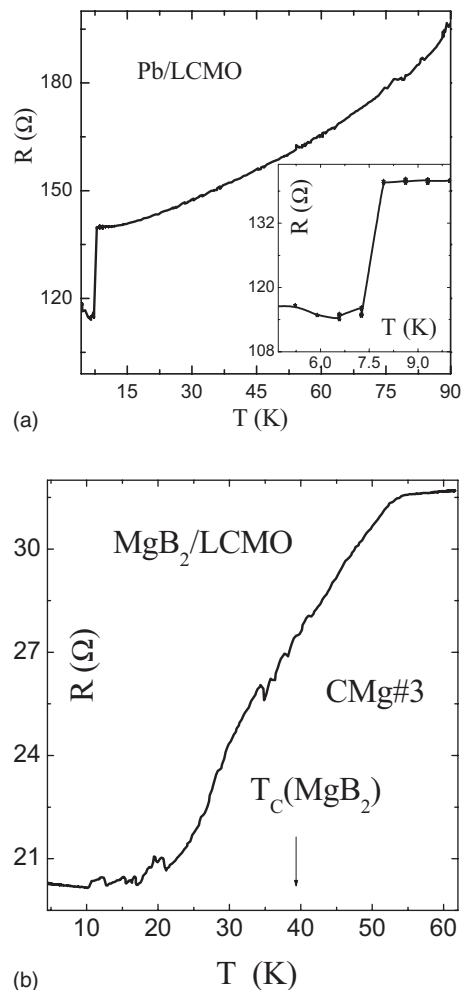

(a)

(b)

FIG. 2. Typical temperature dependence of a resistance of the proximity affected contacts: (a) Pb/LCMO contact (CP#1, reproduced form Ref. 11) (the inset shows a low-temperature region) and (b) MgB$_2$/LCMO contact (CMg#3).

natural to assume that these scattering processes of a "magnetic origin" will cause an increase of the contact's resistance in a normal state. However, the main distinguishing feature of such samples was a quite visible *decrease* of the contact's resistivity just after superconducting transition of Pb or MgB$_2$. We observed pronounced picture of proximity effect on about 10% of the explored PCs. Figure 2 shows an example of the resistance temperature dependence $R(T)$ of the proximity affected Pb/LCMO [Fig. 2(a)] and MgB$_2$/LCMO [Fig. 2(b)] PCs. For the PC on Pb, at $T < 7.2$ K a sharp drop of the contact's resistivity is observed. Reduction of the resistance δR [about 15% for the contact CP#1 shown in Fig. 2(a)] is 2 orders of magnitude larger than it might be expected from the conventional theory of PE for S/F contacts. For the PC on MgB$_2$, decreasing of the contact's resistivity is detected at $T < 37$ K.

At lower temperatures, $T < T_C$(Pb) or T_C(MgB$_2$), the current-voltage characteristic of the contacts exhibits excess current and the differential conductance exhibits excess conductance. In Figs. 3 and 4, both the current-voltage and normalized conductance dependences for good quality proximity affected contacts are presented. We see that like for a
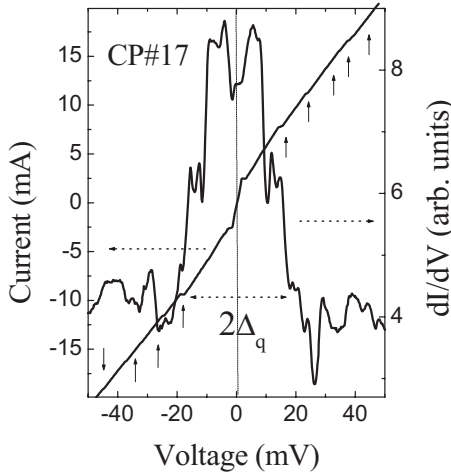
FIG. 3. The current-voltage (I-V) characteristic and normalized conductance for proximity affected contact CP#17; $T = 4.2$ K. The arrows point the current decreasing (jump) in I-V curve which corresponds to a generation of a normal phase section in the superconducting region of LCMO.

conventional AR at S/N interface, the excess current and doubling of the normal-state conductivity have been observed.

The evolution of the AR spectra for proximity affected MgB_2/LCMO contact with changing temperature is illustrated in Fig. 5. One can find similar results for the Pb/LCMO contacts in Fig. 3 of Ref. 11. These data prove that the superconductivity of LCMO is due to superconducting state of Pb or MgB_2. In Fig. 6, the AR spectra for both types of good quality contacts, Pb/LCMO and MgB_2/LCMO, are shown for a comparison.

Before we get into details and models, let us summarize some of the main results (cf. Figs. 2–6). Firstly, in proximity affected Pb/LCMO and MgB_2/LCMO contacts, we observe
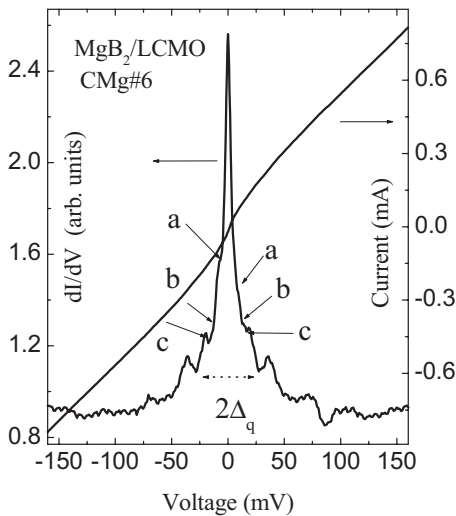

FIG. 4. Normalized conductance spectra and current-voltage characteristic for proximity affected MgB_2/LCMO contact (CMg#6) at 4.2 K. The arrows indicate the energies of the subharmonic gap resonances. See Table I for classification of the resonances.
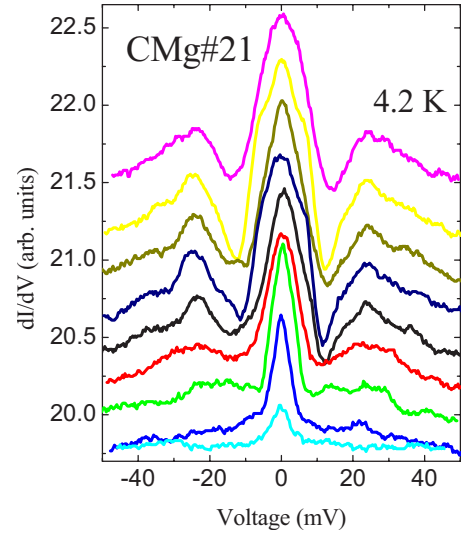

FIG. 5. (Color online) Temperature dependence of the AR spectra for proximity affected MgB_2/LCMO contact (CMg#21). The curves are shifted for clarity; from top to bottom, T (K) $= 4.2, 5.8, 6.4, 7.3, 10.9, 16.5, 20.0, 24.5, 36.0$.

principal facts such as a spectacular drop of the contact's resistance with the onset of the Pb or MgB_2 superconductivity, an excess current, and doubling of the normal-state conductance. Secondly, as was already noted, the AR acts as an alternative conduction channel to the initial quasiparticle current, increasing the normal-state conductance G_N of the point

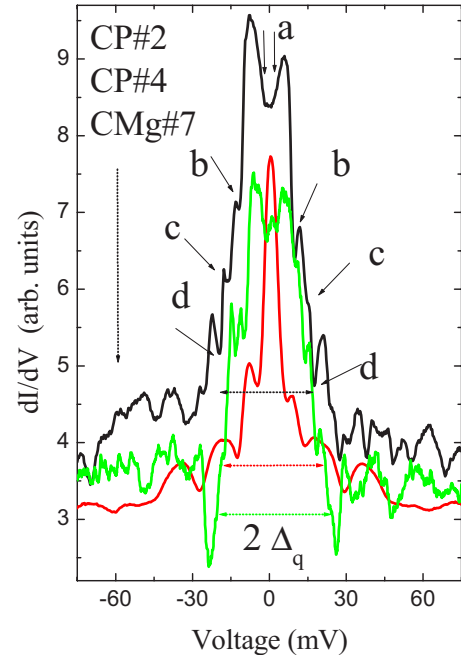FIG. 6. (Color online) Normalized conductance spectra for proximity affected Pb/LCMO point contacts (CP#2 and CP#4, reproduced form Ref. 11) and MgB_2/LCMO contact (CMg#7). The curves are shifted for clarity. The arrows indicate the energies of the subharmonic gap resonances for CP#2 contact. See Table I for classification of the resonances. Δ_q is the apparent proximity induced single-particle gap of the LCMO.

contact for applied voltage $eV < \Delta_q$, where Δ_q is the single-particle gap at the interface. From the data in Figs. 3, 4, and 6 follows an unexpected result: the (apparent) magnitude of proximity induced single-particle gap of the LCMO is much larger than that of the Pb or MgB_2 and may be as large as $\Delta_q \approx 18$–20 meV. Thirdly, by inspecting the AR spectra in Figs. 3, 4, and 6, one can distinguish the peaks (resonances) on which we now concentrate our attention.

Let us start with the subgap region. For voltage $eV < \Delta_q$, a fine structure of the AR spectra is directly visible (and can be classified as described in Sec. IV). This structure is the so-called SGS and manifests itself in a set of downward peaks in the differential conductance that are pointed by labeled arrows in Figs. 4 and 6. Earlier, similar resonances have been observed experimentally and extensively discussed theoretically (see Refs. [12,23–25]). As was explained, these resonances appear at voltages that (roughly) correlate with the energy of quasiparticle gaps divided by integers. What is important for us here is that these resonances can be observed only if *both electrodes are superconductors*. There is no SGS when one of the electrodes is in the normal state.[12,23–25] That is, the observation of the SGS is an additional fact in favor of our conclusion that LCMO is in a superconducting state.

Seldom, for MgB_2/LCMO junctions we observed a large conductance peak in the limit $V \to 0$: $G(0)/G(V) > 2$ (these cases are shown in Figs. 4 and 6). According to the contemporary models (see, for example, Ref. 23 and references therein), for SNS weak links or short constrictions between *two superconductors*, a huge conductance peak $G(0)/G(V) \gg 1$ can be observed at a low voltage if a quasiparticle before reflected inside the junction undergoes $n \sim \Delta/eV$ reflections. This gives an n times larger contribution to the current than a quasiparticle which crosses the junction only once. This fact again confirms our working hypothesis that the HMF electrode (LCMO) is in a superconducting state.

Let us now consider the above-gap region. Inspecting the data in Figs. 3, 4, and 6 for different contacts we see that, in comparison with the subgap region, the character of the contact's conductivity is changed. In general, for all contacts at voltage $eV > \Delta_q$ the conductivity is approximately constant, however, with peak structure. We attributed these peaks to the formation of the so-called "phase-slip lines," the two-dimensional analogue of phase-slip centers.[26,27] Indeed, as is known (see, e.g., Refs. 28 and 29), provided the bias current flowing across the narrow contact is larger than the critical current, a voltage drop between two superconductors appears as soon as the phase slips. That is, the phase may periodically slip by 2π due to formation of a phase-slip center, in which the magnitude of the order parameter oscillates between zero and its maximum value. In a wide superconducting film, the two-dimensional analogue of phase-slip center called phase-slip line may occur.[26,27] In this case, resistivity is associated with the order parameter variation in two dimensions.

In our case, components of the superconducting contact are Pb (or MgB_2) tip and LCMO proximity affected region. For five different superconducting tips (three PCs on Pb and two PCs on MgB_2) with different diameters, the general behavior is common. Taking into account the low magnitude of the LCMO critical current [$I_C \sim 10$ mA (Ref. 5)], we con-

clude that the steplike increase of the contact's resistance is due to a discrete destruction (phase slip) of proximity induced superconducting region of the LCMO. Each current decrease corresponds to a generation of the additional resistance due to appearance of a normal $2L_E$-long section, where L_E is the electrical field penetration length. Directly, the phase slipping points on the current-voltage (I-V) dependence are visible in Fig. 3 (shown by arrows) and one can also find these in Fig. 4 of Ref. 11. We found several features which are characteristic of phase-slip lines.[26,27] (i) The current jumps downward at some critical voltages. (ii) All resistive branches have approximately the same excess current, given by the intersection of their slopes with the current axis. (iii) At high voltage, the I-V curve approaches the normal resistance of the point contact. One can make a crude estimation about the thickness of the LCMO region, L_{LCMO}^{SC}, being in the superconducting state. Indeed, because for each normal-state section the order parameter becomes equal to zero, its thickness is no less than two superconducting coherence lengths of LCMO, $\xi_{LCMO} \approx \hbar v_F / \pi \Delta_{LCMO}$. As was mentioned above, for the majority spin band the Fermi velocity $v_F^{\uparrow}$ is ~10 cm/s, and taking $\Delta_{LCMO} \sim \Delta_q$ one can easily obtain $\xi_{LCMO} \approx$ 20–30 Å. For voltage $eV > \Delta_q$, we definitely detected up to ten peaks for AR spectra of best contacts. Taking into account that the electrical field penetration length L_E is much larger than the superconducting coherence length (see, e.g., Ref. 29), we obtain $L_{LCMO}^{SC} \gg$ 200–300 Å. It means that the proximity affected region is 2 orders larger than it should be due to the conventional PE and is comparable with the one detected in experiments.[5,10]

Systematic character and repeatability of a list of the principal experimental facts suggest that we have observed a general physical phenomenon in transport properties of the proximity affected (Pb or MgB_2)/LCMO contacts.

IV. DISCUSSIONS

At present there are a few models of the subgap transport in the sS/HMF junctions.

To match spin-polarized current in the HMF with spinless current in the S at sS/HMF interface, the magnon-assisted mechanism has been investigated by Tkachov *et al.*,[30] It consists of the simultaneous injection of a Cooper pair from the S (for example, for $V > 0$) and the emission of a magnon inside the HMF. For $V < 0$, the AR is possible only if one electron in the HMF absorbs a magnon to form an intermediate spin-down state before tunneling into the S. The fingerprint of this process is the asymmetric $I(V)$ characteristics of the junction with respect to the base voltage. That is because at $T = 0$, there are no thermally excited magnons and the current is zero for one swing of the bias voltage ($V < 0$) and finite for another ($V > 0$). All the junction's $G(V)$ characteristics we have are symmetric, and thus, the magnon-assisted AR is not the governing transport mechanism in our junctions.

Many-domain state of a ferromagnetic metal opens another opportunity for the subgap transport in the sS/F heterostructures. That is the so-called nonlocal or crossed AR, in which an electron from one magnetic domain is Andreev

reflected as a hole into an adjacent, oppositely polarized, domain while a pair is transmitted into a superconductor.[31–33] To check this possibility, consider the decomposition of the total current through the sS/HMF point contact, j_{tot}, into spin-polarized currents through one, $j_\uparrow$, and another, $j_\downarrow$, domains. Then, we have

$$j_{tot} = j_\uparrow + j_\downarrow = 2j_\downarrow + (j_\uparrow - j_\downarrow) = j_{unpol} + j_{pol}. \quad (3)$$

Here, the unpolarized current j_{unpol} carries no net spin polarization and obeys the conventional AR condition: $\frac{1}{G_N}\frac{d}{dV}j_{unpol}=2$. The current j_{pol} is fully spin polarized and as such is entirely a quasiparticle current. That is, if the interfacial scattering is minimal, then at $(eV, T) \ll \Delta$ for the differential conductance we have $G(0)/G_N = 2(1-P_C)$, where $P_C = (j_\uparrow - j_\downarrow)/(j_\uparrow + j_\downarrow)$ is the spin-polarization magnitude of the total current. In order for the data under consideration to be in agreement with the crossed AR mechanism, the current through the contact has to be unpolarized, $P_C = 0$. It seems improbable that in all the proximity affected contacts, the portion of domains with opposite magnetization is exactly equal. Hence, we find that the crossed AR is not the governing mechanism for charge-carrier transport through $Pb(MgB_2)/LCMO$ junctions.

A more realistic physical picture, it seems to us, is based on the superconducting proximity effect. There are also two qualitatively different models that predict an arising in sS/HMF structures of superconducting triplet correlations with an unusually long penetration length in the ferromagnet due to mutual influence of superconductivity and magnetism. In accordance with Refs. 34 and 35, the appearance of the superconducting *p-wave triplet* pairing with a *finite quasiparticle energy gap* in the HMF metal requires the interplay of two separate interface processes: spin mixing and spin-flip scattering. The spin-rotation effect alone generates at the sS side of the sS/HMF boundary the triplet correlation with "zero spin" component of the form $f_{\uparrow\downarrow} + f_{\downarrow\uparrow}$ (here, $f_{\uparrow\downarrow}$ and $f_{\downarrow\uparrow}$ stand for opposite-spin triplet pair amplitudes). Similar to the wave function of the singlet pair, this component penetrates into the HMF on a short distance $\sim \xi_F$. Additional spin-flip scattering induces both "nonzero spin" triplet components of the pair amplitudes, $f_{\uparrow\uparrow}$ and $f_{\downarrow\downarrow}$, in the sS as well as in the HMF. While spin-scattering centers are chaotically located at the sS/HMF interface, the phase of the triplet correlations is fixed by the phase of the s-wave correlations. That is, coherent triplet pair amplitudes $f_{\uparrow\uparrow}$ and $f_{\downarrow\downarrow}$ are generated in the "parent" s-wave superconductor. Simultaneously, this equal-spin triplet correlation $f_{\uparrow\uparrow}$ (or $f_{\downarrow\downarrow}$) penetrates on an unusually long length $\xi \sim (\hbar D_F/\pi k_B T)^{1/2}$ into the HMF. However, being an odd function of momentum the p-wave triplet condensate function is suppressed by impurity scattering.[36]

Another type of triplet correlations, which can survive strong impurity scattering, has been suggested by the authors of Refs. 37 and 38. In this model, the triplet pairing is described by even in momentum and odd in frequency condensate function and may arise in S/F structures with a nonuniform magnetization in the F. However, for odd in the Matsubara frequency function the magnitude of the triplet superconducting gap equals *zero*. As far as we detect a finite
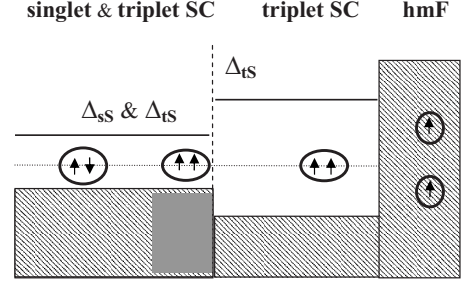

FIG. 7. The semiconductor picture for proximity affected singlet superconductor/half-metallic ferromagnet contact.

proximity induced gap, we think that our data are most likely consistent with the theory.[34,35] (In Ref. 39, a mechanism of induced triplet superconductivity of the F layer is proposed, based on the assumption that both the singlet and triplet types of pairing exist in the S metal. Since Pb and MgB_2 are universally acknowledged to have singlet type of superconductivity, we will not discuss this version here.)

As was mentioned above, the main condition for proximity induced spin-triplet superconducting pairing at sS/HMF interface is the so-called spin-active interface, i.e., the ability of the sS/HMF interface to convert a singlet pair into a triplet one. Unfortunately, theory has not as yet been able to describe in detail the process of conversion. However, qualitative magnetic structure of manganites at present is well understood (see, e.g., Refs. 13 and 14). In particular, the following draft picture for a surface (thickness of a few lattice periods) magnetic structure of manganites has emerged: since the double exchange mechanism is sensitive to a Mn-O-Mn bond state, any structural disorder (oxygen nonstoichiometry, vacancies, stress, etc.) near surface region suppresses the double exchange interaction and leads to a local spin disorder. Another characteristics important for our discussion is that, due to Hund's interaction [for Mn^{3+} the Hund's energy is ~ 1.5 eV Ref. 13], spin disorder serves as strong spin-scattering center for charge carriers.

Assuming that the surface of manganites is a spin-active one, for proximity affected contacts, we suggest that the conditions for the unconventional PE are fulfilled. That is, depending on the local magnetic nonhomogeneity at the sS/LCMO boundary, the LCMO surface causes coherent superconducting triplet correlations which spread over large distance into the manganite's bulk. Simultaneously, triplet correlations extend into the parent sS electrode up to a few coherence lengths from the interface being coupled to the singlet superconducting order parameter (see Fig. 2 of Ref. 34). Following this physics, in Fig. 7 we sketch "a semiconductor picture" of the proximity affected contacts.

The next point concerns a charge transport. We believe that a charge transport through the contact like in Fig. 7 is as follows. Being proximity induced, the supercurrent of equal-spin triplet pairs is continued as a quasiparticle current at the boundary of superconducting and nonsuperconducting phases of the LCMO through the usual AR mechanism, with the excess current and doubling of the normal-state conductance. The main distinguishing feature here is that due to a long-distance PE, we deal with charge transport through

TABLE I. The voltages corresponding to the SGS in Figs. 4 and 6; here, $\Delta_{Pb} \approx 1.4$ meV, $\Delta_{MgB_2} \approx 7$–7.5 meV, and $\Delta_q = \Delta_{LCMO} \approx 18$–$20$ meV.

Label (Fig. 6, CP#2)	Voltage
a	Δ_{Pb}
b	$\Delta_{LCMO}/2$
c	$2\Delta_{LCMO}/3$
d	Δ_{LCMO}
Label (Fig. 4)	Voltage
a	Δ_{MgB_2}
b	$\Delta_{LCMO} - \Delta_{MgB_2}$
c	Δ_{LCMO}

asymmetric S-S′ structure. As was mentioned in Sec. III, the conductance of a metallic contact of two superconductors displays peculiarities (or resonances) at voltage that approximately corresponds to the energy gaps.[12,23–25] Namely, the conductance downward peaks appear at energies Δ_1/n, Δ_2/n, and $(\Delta_1 + \Delta_2)/m$, with $n = 1, 2, 3\ldots$ and $m = 1, 3, 5\ldots$.

We observed pronounced and intense SGS on a few Pb/LCMO contacts. Figures 4 and 6 illustrate the normalized conductance $G(V)/G(0)$ vs voltage dependences for these proximity affected Pb/LCMO contacts (CP#17, CP#2, and CP#4). One can also find additional examples of the AR spectra for proximity affected Pb/LCMO contacts in Ref. 11. For the MgB_2/LCMO proximity affected contacts, SGS is not so intense and it was detected on two samples (see data for CMg#6 and CMg#7 PCs shown in Figs. 4 and 6, respectively). We deal here with a (more than order) difference in superconducting coherence lengths of the superconductors; however, it would be of interest to pursue the origins of this dissimilarity.

According to the data obtained, we can classify the SGS voltages shown in Fig. 4 (for CMg#6 PC) and Fig. 6 (for CP#2 PC) as summarized in Table I (in the figures, the subharmonic gap resonances are pointed by labeled arrows). As it follows, for MgB_2 we observe the largest gap $\Delta_{MgB_2} = 7$–7.5 meV. Theory predicts (see, e.g., Ref. 24) that for intermediate values of Δ_1/Δ_2 a transition from high conductance to low conductance occurs at a fairly well-defined voltage $eV_{cross} \simeq \Delta_2 - \Delta_1$. The differential conductance changes abruptly at eV_{cross} due to the loss of a single AR from the larger-gap superconductor. Indeed, we observed such additional SGS in spectra in Fig. 4 (shown by the arrow "b").

Sometimes, we observed weak downward peak at voltage $eV \simeq 2\Delta_{LCMO}/3$, corresponding to the "forbidden" resonance (shown by the arrow "c" in Fig. 6 for CP#2 contact). This SGS is due to superconducting triplet correlations which spread not only into the manganite's bulk but into the sS as well. Seldom, in the case of perfect contacts, we detected a few forbidden resonances (see the AR spectra at $|eV| < 20$ meV for contacts CP#17 and CP#4 in Figs. 3 and 6, respectively). It may be noted here that trying to operate with transport properties of the system schematically illustrated in Fig. 7, we get in touch with a few open questions of meso-
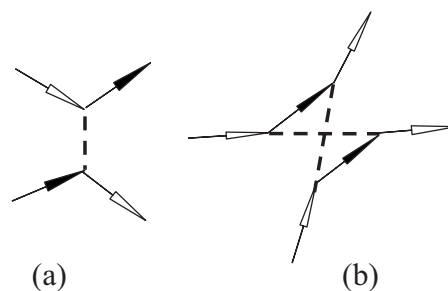

FIG. 8. Electron-electron interaction due to exchange of magnons. Here, the lines with empty (full) arrow correspond to spin-up (spin-down) electrons; the dashed line is magnon.

scopic superconductivity such as the exact mechanisms of conversion of a spin-singlet pair to triplet one at sS-tS (tS refers to triplet superconductor) interface, the interplay between long-range PE and spin-polarized Andreev current, the subgap transport in asymmetric sS-tS weak links, and so on. Quantitative classification of the SGS in proximity affected sS/HMF contacts may be done only after the answers to the questions are clarified. (The discussion of these questions is beyond the scope of this paper.)

At this stage of the investigation, it is possible to assume a scenario that overcomes the contradiction between the proximity induced single-particle gap of LCMO and the superconducting gap of Pb or MgB_2. We suggest that the large value of the proximity induced gap may be expected if the HMF (manganite) is thermodynamically very close to triplet p-wave superconducting state. That is at low temperature, the local triplet superconducting fluctuations are essentially sustained in LCMO and the singlet superconductor only induces *the phase coherency* of a superconducting state. The situation here may be similar to superconducting properties of strontium ruthenate Sr_2RuO_4.[40] Convincing experimental data have been obtained in favor of the spin-triplet p-wave superconductivity of clean Sr_2RuO_4. However, the superconductivity in impure Sr_2RuO_4 has not been observed. Also, the intrinsic superconducting critical temperature of Sr_2RuO_4 is 1.5 K. However, it was found that in the Sr_2RuO_4-Ru eutectic system, the T_C was enhanced up to 3 K.[41] As far as the Ru inclusions are superconducting due to the proximity effect, 3 K phase superconductivity is now considered to be essentially sustained in Sr_2RuO_4.[40–43]

Because of phase separation, the half-metallic ferromagnetic state of manganites is intrinsically "impure" case, i.e., the "clean" limit cannot physically be realized for spin-polarized metallic phase of the materials. At the same time, the superconducting fluctuations of p-wave symmetry may be quite strong due to, for example, the mechanism proposed by Akhiezer and Pomeranchuk.[44] For a ferromagnetic metal, these authors show that there is an additional attraction between conducting electrons due to exchange of the spin waves (magnons) [see diagrammatic presentation of this mechanism in Fig. 8(a)]. This interaction is much larger than the usual electron-phonon interaction and corresponds to p-wave symmetry of the triplet correlation function with large quasiparticle gap. It is easy to show that (in the second order) an electron-electron interaction due to exchange of

magnons gives triplet pairs with nonzero-spin component [see Fig. 8(b)]. Proximity induced *p*-wave triplet correlations may quench these intrinsic superconducting phase fluctuations that will result in the long-range *coherent triplet superconducting state* of manganite.

Let us also note that the idea of instability against formation of *p*-wave triplet pairs, based on the spin-dependent interaction arising from spin fluctuation exchange, was intensively discussed earlier in relation to the *A* and *B* phases of liquid [3]He (see review[45]). An interesting scenario of spin-mediated *p*-wave triplet superconductivity in ferromagnetic half metals has been considered recently in Ref. [46]. In the model under consideration, the superconducting critical temperature and the gap energy for the *p*-wave triplet equal-spin pairing are actually increased by an exchange splitting. It would be of interest to pursue this model further.

Naively, using the well known BCS relation between superconducting energy gap and superconducting critical temperature, one can restore the T_C for LCMO: $T_C = \Delta_{LCMO}/1.76 \sim 100$ K. This magnitude of T_C is comparable to those of high-T_C superconductors. As is well known, several theoretical models and numerous experimental data (see, e.g., Ref. [47] and references therein) suggest that strong (antiferro)magnetic correlations in a superconducting state are an intrinsic feature of cuprate high-T_C materials. Our suggestion about superconducting fluctuations in half-metallic manganites adds a similarity between these materials and high-T_C cuprates (in addition to those known such as phase separation, pseudogap band structure, nesting properties of the Fermi surface, etc.). Curiously, the scenario of a "high-T_C superconductivity in doped manganites" was also proposed recently by Baskaran.[48] The author, using a body of already existing theoretical and experimental insights in cuprates and manganites (see, in particular, Refs. [49] and [50]), suggests that in the fully spin-polarized metallic phase of manganites there is a "latent high-T_C superconductivity" with a (real) spin triplet, pseudo-spin-singlet *d*-wave order parameter. (Orbital degree of freedom offers a possibility to have *d*-wave spin triplet, still maintaining the overall antisymmetry of the wave function.) The magnitude of the superconducting gap depends on doping. However, due to the pseudo-spin-flip processes, superconducting critical temperature gets suppressed to zero. An interesting consequence of the proposal[48] is a long-distance superconducting proximity effect due to the AR with pseudo-spin-reversion.

V. SUMMARY

To clarify mutual influence of spinless supercurrent in a singlet superconductor and spin-polarized current in a half-metallic ferromagnet, we investigated a subgap transport in singlet superconductor (Pb or MgB$_2$)-half-metallic ferromagnet (La$_{0.65}$Ca$_{0.35}$MnO$_3$) point contacts. In the contacts, which we distinguish as proximity affected ones, a few specific effects have been detected. In particular, we have observed the following: a spectacular drop in the resistance of the contacts at the onset of the Pb (MgB$_2$) superconductivity; typical for S/normal nonmagnetic metal contacts, excess current and doubling of the normal-state conductance; and the subharmonic gap structure due to multiple Andreev reflections. Character of the differential conductance vs voltage dependence in such contacts corresponds to the Andreev spectra with proximity induced quasiparticle energy gap much larger than that of the superconducting injectors (Pb or MgB$_2$). Possible mechanisms of the subgap current in a superconductor/half-metallic ferromagnet junction have been discussed. The very distinct Andreev reflection characteristics of the proximity affected contacts observed by us suggest that local triplet superconductivity is essentially sustained in half-metallic phase of LCMO.

However, the large spread in the Andreev spectra observed in the experiments shows that the formation of the interface plays a crucial role. At present, it is hard to make a quantitative comparison of the experimental results to theory. Answers to a few important questions of the theory should be obtained in advance. Although some details may be incorrect, we believe that a qualitative picture is founded and provides an attractive explanation for a different kind of proximity effect concerned with magnetism of manganese oxides.

[1] A. F. Andreev, Sov. Phys. JETP **19**, 1228 (1964).

[2] G. J. Strijkers, Y. Ji, F. Y. Yang, C. L. Chien, and J. M. Byers, Phys. Rev. B **63**, 104510 (2001); B. Pannetier and H. Courtois, J. Low Temp. Phys. **118**, 599 (2000); P. C. van Son, H. van Kempen, and P. Wyder, Phys. Rev. Lett. **59**, 2226 (1987); G. E. Blonder and M. Tinkham, Phys. Rev. B **27**, 112 (1983).

[3] G. E. Blonder, M. Tinkham, and T. M. Klapwijk, Phys. Rev. B **25**, 4515 (1982).

[4] M. J. M. de Jong and C. W. J. Beenakker, Phys. Rev. Lett. **74**, 1657 (1995).

[5] M. Kasai, Y. Kanke, T. Ohno, and Y. Kozono, J. Appl. Phys. **72**, 5344 (1992).

[6] V. T. Petrashov, I. A. Sosnin, I. Cox, A. Parsons, and C. Troadec, Phys. Rev. Lett. **83**, 3281 (1999).

[7] Z. Sefrioui, D. Arias, V. Peňa, J. E. Villegas, M. Varela, P. Prieto, C. Leon, J. L. Martinez, and J. Santamaria, Phys. Rev. B **67**, 214511 (2003).

[8] V. Peňa, Z. Sefrioui, D. Arias, C. Leon, J. Santamaria, M. Varela, S. J. Pennycook, and J. L. Martinez, Phys. Rev. B **69**, 224502 (2004).

[9] F. S. Bergeret, A. F. Volkov, and K. B. Efetov, Rev. Mod. Phys. **77**, 1321 (2005).

[10] R. S. Keizer, S. T. B. Goennenwein, T. M. Klapwijk, G. Miao, G. Xiao, and A. Gupta, Nature (London) **439**, 825 (2006).

[11] V. N. Krivoruchko, V. Yu. Tarenkov, A. I. D'yachenko, and V. N. Varyukhin, Europhys. Lett. **75**, 294 (2006).

[12] T. M. Klapwijk, G. E. Blonder, and M. Tinkham, Physica B & C **109**, 1657 (1982).

[13] E. Dagotto, T. Hotta, and A. Moreo, Phys. Rep. **344**, 1 (2001).

[14] V. M. Loktev and Yu. G. Pogorelov, Low Temp. Phys. **26**, 171 (2000).

[15] M. Xu, H. Kitazawa, Y. Takano, J. Ye, K. Nishida, H. Abe, A. Matsushita, N. Tsujii, and G. Kido, Appl. Phys. Lett. **79**, 2779 (2001); S. Suoma, Y. Machida, T. Sato, T. Takahashi, H. Matsui, S.-C. Wang, H. Ding, A. Kaminski, J. C. Campuzano, S. Sasaki, and K. Kadowaki, Nature (London) **423**, 65 (2003).

[16] A. Hoffmann, S. G. E. te Velthuis, Z. Sefrioui, J. Santamaria, M. R. Fitzsimmons, S. Park, and M. Varela, Phys. Rev. B **72**, 140407(R) (2005).

[17] G. Wexler, Proc. Phys. Soc. London **89**, 927 (1966).

[18] J. Mitra, A. K. Raychaudhuri, Ya. M. Mukovskii, and D. Shulyatev, Phys. Rev. B **68**, 134428 (2003).

[19] W. E. Pickett and D. J. Singh, Phys. Rev. B **53**, 1146 (1996).

[20] Yu. V. Sharvin, Sov. Phys. JETP **21**, 655 (1965).

[21] R. J. Soulen, Jr., J. M. Byers, M. S. Osofsky, B. Nadgorny, T. Ambrose, S. F. Cheng, P. R. Broussard, C. T. Tanaka, J. Novak, J. S. Moodera, A. Barry, and J. M. D. Coey, Science **282**, 85 (1998).

[22] A. I. D'yachenko, V. A. D'yachenko, V. Yu. Tarenkov, and V. N. Krivoruchko, Phys. Solid State **48**, 432 (2006).

[23] U. Gunsenheimer and A. D. Zaikin, Phys. Rev. B **50**, 6317 (1994).

[24] M. Hurd, S. Datta, and P. F. Bagwell, Phys. Rev. B **54**, 6557 (1996).

[25] G. Arnold, J. Low Temp. Phys. **68**, 1 (1987).

[26] I. M. Dmitrenko, Low Temp. Phys. **22**, 686 (1996).

[27] A. G. Sivakov, A. M. Glukhov, A. N. Omelyanchouk, Y. Koval, P. Müller, and A. V. Ustinov, Phys. Rev. Lett. **91**, 267001 (2003).

[28] M. Tinkham, *Introduction to Superconductivity*, 2nd ed.

[29] (McGraw-Hill, New York, 1996).

[29] K. K. Likharev, Rev. Mod. Phys. **51**, 101 (1979).

[30] G. Tkachov, E. McCann, and V. Fal'ko, Phys. Rev. B **65**, 024519 (2001).

[31] G. Deutscher and D. Feinberg, Appl. Phys. Lett. **76**, 487 (2000).

[32] D. Beckmann, H. B. Weber, and H. v. Löhneysen, Phys. Rev. Lett. **93**, 197003 (2004).

[33] P. Aronov and G. Koren, Phys. Rev. B **72**, 184515 (2005).

[34] M. Eschrig, J. Kopu, J. C. Cuevas, and G. Schön, Phys. Rev. Lett. **90**, 137003 (2003).

[35] T. Champel and M. Eschrig, Phys. Rev. B **72**, 054523 (2005).

[36] A. I. Larkin, JETP Lett. **2**, 130 (1965).

[37] F. S. Bergeret, A. F. Volkov, and K. B. Efetov, Phys. Rev. Lett. **86**, 4096 (2001).

[38] A. Kadigrobov, R. I. Skekhter, and M. Jonson, Europhys. Lett. **54**, 394 (2001).

[39] V. M. Edelstein, Phys. Rev. B **67**, 020505(R) (2003).

[40] I. Eremin, D. Manske, S. G. Ovchinnikov, and J. F. Annet, Ann. Phys. **13**, 149 (2004) and references therein.

[41] Y. Maeno, T. Ando, Y. Mori, E. Ohmichi, S. Ikeda, S. NishiZaki, and S. Nakatsuji, Phys. Rev. Lett. **81**, 3765 (1998).

[42] Z. Q. Mao, K. D. Nelson, R. Jin, Y. Liu, and Y. Maeno, Phys. Rev. Lett. **87**, 037003 (2001).

[43] H. Yaguchi, M. Wada, T. Akima, Y. Maeno, and T. Ishiguro, Phys. Rev. B **67**, 214519 (2003).

[44] A. Akhiezer and I. Pomeranchuk, Sov. Phys. JETP **36**, 859 (1959).

[45] A. J. Leggett, Rev. Mod. Phys. **47**, 331 (1975).

[46] B. J. Powel, J. F. Annet, and B. L. Györffy, J. Phys. A **36**, 9289 (2003).

[47] A. P. Kampf, Phys. Rep. **249**, 219 (1994).

[48] G. Baskaran, e-print arXiv:cond-mat/0607369.

[49] W. E. Pickett and D. J. Singh, Phys. Rev. B **55**, R8642 (1997).

[50] E. A. Livesay, R. N. West, S. B. Dugdale, G. Santi, and T. Jarlborg, J. Phys.: Condens. Matter **11**, L279 (1999).